Efficient Fully-Digital Beamformer for Very-Large Non-Uniform Arrays using Hexagonal Transformations

Juan Carlos Merlano Duncan, Juan Andres Vasquez-Peralvo, Vibhun Singh, Vu Nguyen Ha, Luis Manuel Garces-Socarras, Ti Ti Nguyen, Raudel Cuiman, Jorge Luis Gonzalez-Rios, Symeon Chatzinotas, and Björn Ottersten
Interdisciplinary Centre for Security, Reliability and Trust (SnT), *University of Luxembourg*, Luxembourg
{juan.duncan, juan.vasquez, vibhun.singh, vu-nguyen.ha, luis.garces, titi.nguyen, raudel.cuiman, jorge.gonzalez, symeon.chatzinotas, bjorn.ottersten}@uni.lu

***Abstract*—Digital beamforming is a critical technology for next-generation satellite communications. Conventional solutions in current missions primarily rely on hybrid analog-digital architectures due to the significant power consumption challenges of a fully-digital implementation. For future systems, Fast Fourier Transform (FFT)-based beamforming has been proposed as an efficient digital alternative, especially for managing many beams. However, the use of a FFT beamforming alone is not compatible with non-uniform antennas and beams. This inflexibility poses a significant challenge for modern satellite systems, which require beam reconfigurability to accommodate changing traffic demands. The Non-Uniform FFT (NUFFT) offers the needed flexibility for non-uniform grids, but it involves higher computational costs due to extra processing steps. This paper presents a new method to lower this cost by mapping the spatial samples onto a hexagonal grid instead of the traditional Cartesian grid. Taking advantage of the efficient 2D sampling efficiency of the hexagonal lattice, our approach uses circularly symmetric windows more effectively. This efficiency allows for more accurate signal reconstruction with fewer operations. The hexagonal transformation offers a more power-efficient and adaptable way to achieve real-time, dynamic beam steering required in advanced satellite systems.**

***Index Terms*—Digital beamforming, non-uniform arrays, NUFFT, hexagonal sampling, satellite communications, FFT.**

I. Introduction

The demand for higher throughput and greater flexibility in satellite communication (SatCom) systems has driven significant interest in fully-digital beamforming architectures [1]. In contrast to current-generation systems, which predominantly use power-efficient but less flexible hybrid analog-digital beamformers, future payloads are envisioned to be fully digital. This transition promises unprecedented reconfigurability in generating and steering a massive number of beams, which is essential for meeting dynamic traffic demands [2]. However, the main obstacle to realizing fully-digital payloads remains the high power consumption and computational complexity associated with processing signals for very-large antenna arrays.

This work is being carried out within the ARTES 4.0 CORE COMPETITIVENESS GENERIC PROGRAMME LINE Component A: ADVANCED TECHNOLOGY under ESA Contract no 4000145082/24/NL/FGL and funded by the European Space Agency.

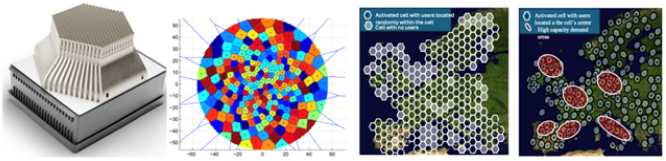

Fig. 1: Illustration of non-uniform antenna arrays and reconfigurable beam lattices for satellite coverage [8] [9].

An effective method to reduce the computational load of digital beamforming (DB) is to leverage the Fast Fourier Transform (FFT) [3]. For a uniform planar array generating a corresponding uniform grid of beams, the beamforming operation is equivalent to a 2D Discrete Fourier Transform (DFT), which can be computed efficiently using a 2D-FFT algorithm. This approach reduces the complexity from $\mathcal{O}(N^2)$ to $\mathcal{O}(N \log N)$, where N is the total number of antenna elements [4], [5]. This computational saving makes FFT-based beamforming a compelling solution for future systems with thousands of beams and array elements [6].

However, the strict reliance of the FFT on a uniform structure for both the antenna elements and the beam positions imposes a fundamental limitation. Modern SatCom systems, particularly those in Non-Geostationary Satellite Orbits (NGSO), require the ability to dynamically reconfigure beam patterns to adapt to changing user density and traffic hotspots [7]. Furthermore, the use of non-uniform arrays, such as sparse or thinned lattices, is desirable for reducing the total number of radiating elements and controlling sidelobe levels [8]. The inherent rigidity of the standard FFT algorithm makes it incompatible with these requirements.

The Non-Uniform Fast Fourier Transform (NUFFT) framework was developed to bridge this gap, enabling the application of FFT-level efficiency to non-uniformly sampled data [10], [11]. The NUFFT framework is generally categorized into three distinct problems. The **Type 1 NUFFT** evaluates

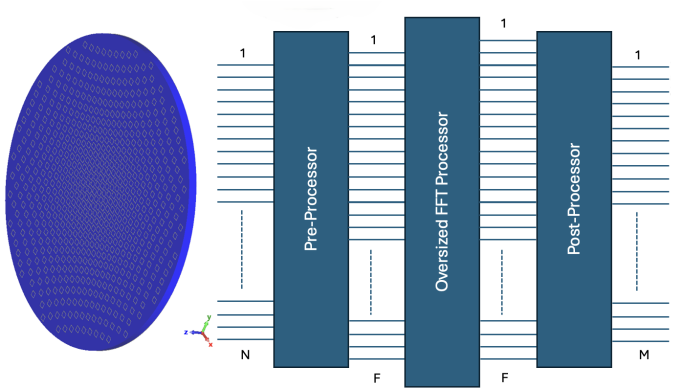

Fig. 2: Conceptual block diagram of a conventional NUFFT-based beamformer, showing the pre-processing, FFT, and post-processing stages. This architecture forms the baseline against which our proposed hexagonal transformation method is compared.

the transform at non-uniform outputs from uniform spatial data. Conversely, the **Type 2 NUFFT**, the adjoint of Type 1, evaluates the transform at uniform frequencies from non-uniform inputs. The most general case, the **Type 3 NUFFT**, handles both non-uniform input and ouput samples. Our proposed approach is suitable for all cases and is of particular interest for the Type-3 operation. Table I shows the mapping of these three NUFFT types into the actual transmission and reception scenarios. The core of these NUFFT algorithms is the interpolation step, which relies on convolving the data with a carefully chosen windowing function at the non-uniform domain and then applying a scaling function at the uniform domain. Fig. 2 shows a pictorial description of the processing chain for the reception operation using a non-uniform array. The pre-processing block is in charge of the interpolation of the non-uniformly sampled data, and the post-processing block does the scaling in accordance with the interpolation function in use, being a sampled version of the Fourier transform of the interpolation function. Different kinds of kernel interpolation functions have been proposed in the literature. A common choice for this function is the Kaiser-Bessel window, which is known to be optimal from a least mean square error reconstruction criterion [12], [13]. For a 1D case, the Kaiser-Bessel window is given by:

$$\phi(x) = \frac{I_0\left(\beta\sqrt{1-(2x/W)^2}\right)}{I_0(\beta)}, \quad |x| \le W/2, \qquad (1)$$

where W is the window width or support, $I_0(\cdot)$ is the zeroth-order modified Bessel function of the first kind, and β is a shape parameter that controls the trade-off between main-lobe width and side-lobe level. For 2D problems on a Cartesian grid, this window is typically applied separately along each dimension. While effective, this separable application is sub-optimal for circularly band-limited signals and motivates our proposed approach. In this paper, we propose an approach that significantly improves the accuracy of the DB process while keeping the same computational costs as the Cartesian NUFFT. The key contribution is the use of a hexagonal grid for the intermediate uniform domain, instead of the conventional Cartesian (rectangular) grid. A hexagonal lattice is known to be the most efficient method for sampling 2D signals. By mapping the non-uniform data to a hexagonal grid, we can use circularly symmetric windowing functions more effectively, leading to a more accurate signal reconstruction with fewer computational operations. This hexagonal transformation offers a more power-efficient pathway to achieving the full flexibility required for next-generation, very-large non-uniform arrays. The remainder of this paper is organized as follows. Section II describes the system model for DB with non-uniform arrays. Section III details the proposed algorithm based on hexagonal transformations. Section IV presents a performance assessment and comparison with conventional methods. Finally, Section V concludes the paper.

II. System Model

We model an active planar antenna array for a satellite communications payload, designed to operate in both transmission (Tx) and reception (Rx) modes. A key aspect of this model is its ability to handle non-uniformity in both the antenna element positions and the beam placement. While the physical locations of the array elements are fixed after deployment, the grid of beams is desired to be fully reconfigurable during operation to adapt to changing traffic conditions. The array is composed of N radiating elements located at arbitrary, non-uniform positions in the xy-plane. The position of the n-th element is given by the vector $\mathbf{p}_n = (x_n, y_n)$ for $n = 0, 1, \ldots, N-1$. An example of such a geometry is shown in Fig. 3, which illustrates a Density-Tapered aperiodic Array obtained through a density-driven synthesis approach [14]. While this particular configuration is used as a reference, the proposed beamforming technique is general and applicable to other types of non-uniform arrays. The array is required to form M simultaneous beams, each pointing towards a specific direction. These directions are also potentially non-uniform and are defined in terms of their direction cosines (u_m, v_m), where $u = \sin\theta\cos\phi$ and $v = \sin\theta\sin\phi$. The wave vector for the m-th beam is thus $\mathbf{k}_m = \frac{2\pi}{\lambda}(u_m, v_m)$, where λ is the wavelength.

For the next analysis, we will focus on the receive (Rx) case without loss of generality, as the principles and performance trade-offs are directly applicable to the receive (Rx) case through reciprocity. The overall beamforming operation can be represented by the matrix-vector multiplication:

$$\mathbf{x} = \mathbf{W}\mathbf{r}, \qquad (2)$$

where $\mathbf{r} \in \mathbb{C}^M$ is the vector of received complex values in each of the N antennas, $\mathbf{x} \in \mathbb{C}^M$ is the vector of M recovered signals, and $\mathbf{W} \in \mathbb{C}^{M\times N}$ is the beamforming matrix. The elements of $\mathbf{W}$ are given by:

$$[\mathbf{W}]_{m,n} = e^{-j\mathbf{k}_m\cdot\mathbf{r}_n} = e^{-j\frac{2\pi}{\lambda}(u_m x_n + v_m y_n)}. \qquad (3)$$

TABLE I: Classification of Beamforming Scenarios according to NUFFT Type Definitions

	Type 1 NUFFT (Uniform Input → Non-Uniform Output)	**Type 2 NUFFT** (Non-Uniform Input → Uniform Output)	**Type 3 NUFFT** (Non-Uniform Input → Non-Uniform Output)
Reception (Rx)	Uniform Array (Input) → Non-Uniform Beams (Output)	Non-Uniform Array (Input) → Uniform Beams (Output)	Non-Uniform Array (Input) → Non-Uniform Beams (Output)
Transmission (Tx)	Uniform Beams (Input) → Non-Uniform Array (Output)	Non-Uniform Beams (Input) → Uniform Array (Output)	Non-Uniform Beams (Input) → Non-Uniform Array (Output)

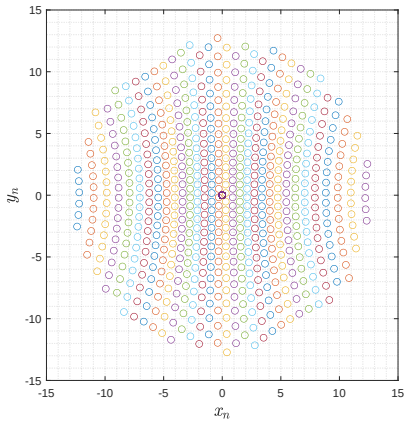

Fig. 3: Example of a Density-Tapered aperiodic Array geometry containing **688 unit-cell** antennas. The shown x and y values are normalized to the wavelength.

Remark 1. *The direct computation of (2) has a complexity of $\mathcal{O}(MN)$, which is prohibitive for the large values of M and N envisioned for future systems.*

The primary goal of the beamforming network is to maximize the signal quality for each user. A key metric for this is the Signal-to-Interference Ratio (SIR). Let us consider a user intended to be served by the k-th beam, located at the direction (u_k, v_k). The signal power received by this user is proportional to the squared magnitude of the array factor of the k-th beam evaluated at its pointing direction. The interference is the undesired power contribution from all other beams, $m \neq k$, at that same location. Assuming the data symbols transmitted on each beam are independent and have equal power, the SIR for user k can be expressed as

$$\text{SIR}_k = \frac{|A_k(u_k, v_k)|^2}{\sum_{m \neq k} |A_m(u_k, v_k)|^2}, \tag{4}$$

where $A_m(u, v)$ is the far-field array factor of the m-th beam evaluated at direction (u, v), which is given by:

$$A_m(u, v) = \sum_{n=0}^{N-1} e^{-j\frac{2\pi}{\lambda}[(u_m - u)x_n + (v_m - v)y_n]}. \tag{5}$$

Given the computational barrier of direct computation, expressed in Remark 1, efficient algorithms like the NUFFT are necessary. The following section details our proposed enhancement to the conventional NUFFT framework to further improve its efficiency.

III. Proposed Algorithm for Non-Uniform Array and Beam Lattices

The conventional NUFFT approach, which maps non-uniform data onto a Cartesian grid, suffers from inefficiencies when dealing with signals whose spectral support is approximately circular, as is common in antenna array theory. The use of separable windowing functions on a square grid requires a higher sampling density than theoretically necessary, leading to increased computational cost in the FFT stage. The core of the proposed method is to map the non-uniform spatial samples (from the array elements or for the beams) onto a regular, oversampled **hexagonal grid**. This process can be conceptualized in two steps.

1) Step One: A set of base points on a standard rectangular grid (X_0, Y_0) can be defined with spacings d_x and d_y:

$$\begin{aligned} X_0 &= k d_x \lambda_0, \quad \forall k \in \{1, \ldots, M_x\}, \\ Y_0 &= l d_y \lambda_0, \quad \forall l \in \{1, \ldots, N_y\}, \end{aligned} \tag{6}$$

where λ_0 is a reference wavelength, and M_x, N_y define the grid size.

2) Step Two: A linear matrix transformation translates the rectangular coordinates into a hexagonal lattice. The resulting hexagonal grid points (X, Y) are given by:

$$\begin{bmatrix} X \\ Y \end{bmatrix} = \begin{bmatrix} \sqrt{3}/2 & 0 \\ -0.5 & 1 \end{bmatrix} \begin{bmatrix} X_0 \\ Y_0 \end{bmatrix}. \tag{7}$$

Once the target uniform hexagonal grid is defined, the interpolation from the non-uniform sample points is performed. For each non-uniform point, we identify the nearest hexagonal grid points and distribute its value among them using a circularly symmetric windowing function, such as a 2D version of the Kaiser-Bessel window defined in (1).

Remark 2. *After the non-uniform data has been gridded onto the hexagonal lattice, the system processes the samples with a standard 2D FFT, thus preserving the computational advantages. The final step involves a deconvolution in the transform domain to compensate for the effect of the interpolation window, similar to the conventional NUFFT process.*

IV. Performance Assessment

In this section, we evaluate the performance of the proposed hexagonal grid-based NUFFT beamformer against a conventional NUFFT implementation that uses a Cartesian (square) grid. The primary goal is to demonstrate that for an identical computational budget, our hexagonal approach yields

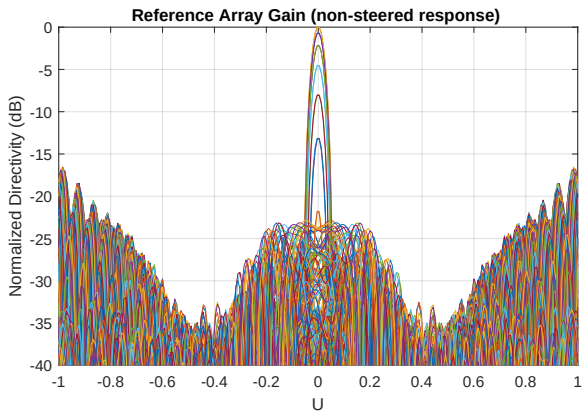

Fig. 4: Beamforming pattern of the aperiodic array of Figure 3 when no steering is applied.

a superior beamforming pattern. To ensure a fair comparison, the computational cost for both methods was kept the same. Both NUFFT implementations utilize a **64x64-point 2D-FFT** for the core transform. The interpolation stage for both methods is based on a convolution using a kernel derived from a Kaiser-Bessel function. For each non-uniform sample, this continuous interpolation function is discretized over a **13x13 support grid**. The smallest coefficients within this support are then nullified, leaving **85 valid points** that are used to distribute the signal's value onto the neighboring uniform grid points.

To establish an ideal benchmark, we first compute the reference radiation pattern using a brute-force calculation of the Array Factor, as defined by the double summation in (5). This pattern, shown in Fig. 4, represents the "ground truth" directivity and serves as the benchmark against which we measure the accuracy of both NUFFT implementations.

The core of our performance evaluation is presented in Fig. 5, which provides a direct comparison of the same beam generated by both methods. Because the underlying uniform grids are different, the beam indices are not identical (1,14 for the square grid vs. 1,16 for the hexagonal); however, care was taken to ensure both beams point to the same spatial direction in the uv-plane.

Figures 5a and 5b illustrate the full 3D directivity patterns. While both methods successfully reconstruct the main beam, the key difference lies in the quality of this reconstruction. A more detailed analysis is provided by the 2D cross-sections in Figures 5c and 5d. These plots clearly show that for the same computational cost, the hexagonal grid approach results in a cleaner beam pattern with lower sidelobe levels and a more circularly symmetric main lobe. This demonstrates that the hexagonal lattice, due to its superior 2D sampling properties, allows the interpolation kernel to reconstruct the signal more accurately. The advantages of these results are further increased because the parts that are most affected by Side Lobe Level (SLL) are in the middle of the pattern, but the designed base radiation pattern will leave the high interference components out of the field of view.

V. Conclusions

This paper proposes a hexagonally transformed NUFFT that significantly improves the quality of digital beamforming in non-uniform arrays without increasing computational cost. In particular, it showcased that for an identical computational cost—specifically, using the same size 64x64 2D-FFT and the same 85-point interpolation kernel derived from a 13x13 support grid—the proposed hexagonal method yields a beamforming pattern with superior quality compared to the conventional Cartesian grid approach.

We obtain the results for a Type-2 NUFFT in reception, but the results can be extrapolated to the Type-1 in transmission and can be extended into a Type-3 operation, where both antennas and beams can be non-uniformly placed. While the results are based on a specific antenna geometry, they strongly suggest that the conclusions are applicable to other configurations.

The fundamental advantage of the hexagonal grid lies in its inherent efficiency for sampling 2D space. For the same number of points, the area of the hexagonal grid's unit cell is $\sqrt{3}/2$ times that of the Cartesian grid's unit square. This results in an effective sampling density that is approximately 15.5% higher. This increased density allows the interpolation process to comply more effectively with the Nyquist sampling criterion, leading to a more accurate signal reconstruction. Consequently, the distortions that typically appear at high angular frequencies in NUFFT implementations are significantly reduced.

This improved accuracy provides two key benefits. First, it enables the generation of a larger number of non-distorted beams across the field of view compared to the Cartesian method under the same computational constraints. Second, the resulting beam patterns exhibit lower sidelobe levels, which is critical for managing interference and SIR levels.

The advantages are further enhanced in practical systems, as the designed base radiation pattern of the antenna can ensure that the highest interference components are placed outside the operational field of view.

Looking forward, the enhanced stability and efficiency of the hexagonal grid open the possibility for future research into novel interpolation windows that were previously discarded due to numerical instabilities on Cartesian grids. The development of such new interpolation kernels could lead to implementations requiring a much smaller number of operations. This would directly translate into a significant reduction in computational cost, a critical advantage for future onboard satellite missions where power and physical area are extremely limited and expensive resources.

References

[1] A. M. Elbir, K. V. Mishra, S. A. Vorobyov, and R. W. Heath, Jr., "Twenty-five years of advances in beamforming: From convex and nonconvex optimization to learning techniques," *IEEE Transactions on Signal Processing*, vol. 71, pp. 1234–1256, 2023.

[2] R. De Gaudenzi, P. Angeletti, D. Petrolati, and E. Re, "Future technologies for very high throughput satellite systems," *International Journal on Satellite Communications and Networking*, vol. 38, no. 2, pp. 141–161, Mar./Apr. 2020.

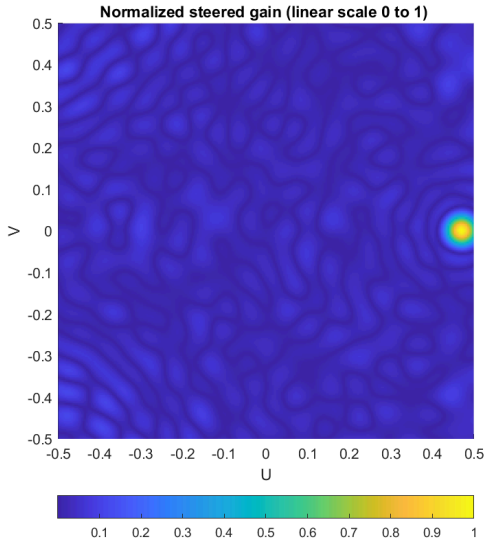

(a) Square grid for the FFT processing in the U-V plane

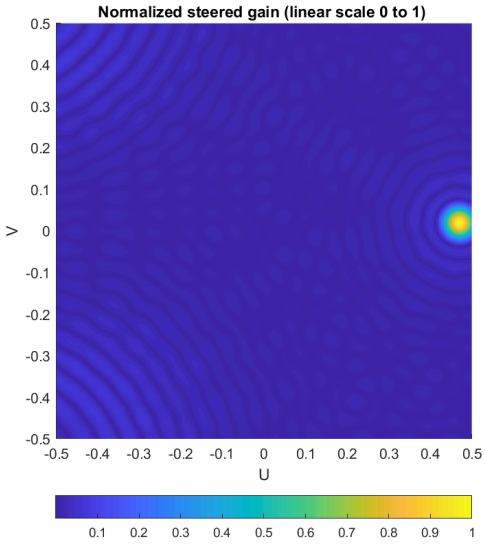

(b) Hexagonal grid for the FFT processing in the U-V plane

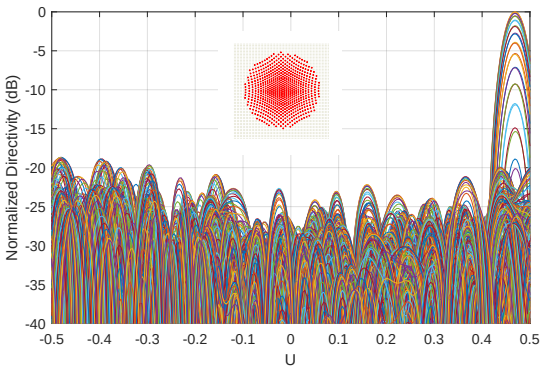

(c) Square grid. FFT beam index: 1,14

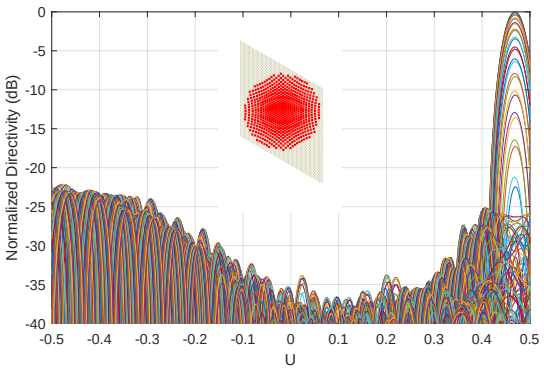

(d) Hexagonal grid. FFT beam index: 1,16

Fig. 5: Comparison of the beamforming patterns in Rx for square and hexagonal FFT grids. For a 2D FFT size of 64 points.

[3] P. Barton, "Digital beam forming for radar," *Proc. Inst. Electr. Eng. F. Commun. Radar Signal Process.*, vol. 127, no. 4, pp. 266–277, Aug. 1980.

[4] L. M. Garcés-Socarrás, J. L. González-Rios, R. Palisetty, R. Cuiman, V. N. Ha, J. A. Vásquez-Peralvo, G. Eappen, T. T. Nguyen, J. C. M. Duncan, S. Chatzinotas, B. Ottersten, C. L. Marcos, A. Coskun, S. King, S. D'Addio, and P. Angeletti, "Efficient digital beamforming for satellite payloads using a 2d fft-based parallel architecture," in *2025 IEEE International Symposium on Circuits and Systems (ISCAS)*, 2025, pp. 1–5.

[5] R. Palisetty, L. M. Garces-Socarras, W. A. Martins, J. L. Gonzalez-Rios, J. A. Vasquez-Peralvo, V. N. Ha, J. C. M. Duncan, S. Chatzinotas, and B. Ottersten, "Area-power analysis of fft based digital beamforming for geo, meo, and leo scenarios," in *2022 IEEE 95th Vehicular Technology Conference: (VTC2022-Spring)*, June 2022, pp. 1–5.

[6] P. Angeletti, "Multiple beams from planar arrays," *IEEE Transactions on Antennas and Propagation*, vol. 62, no. 4, pp. 1750–1761, Apr. 2014.

[7] P. Angeletti and R. De Gaudenzi, "Heuristic radio resource management for massive MIMO in satellite broadband communication networks," *IEEE Access*, vol. 9, pp. 147 164–147 190, Oct. 2021.

[8] M. C. Vigano, G. Toso, G. Caille, C. Mangenot, and H. Lager, "Sunflower array antenna with adjustable density taper," *Hindawi Special Issue on Active Antennas for Satellite Applications*, 2009.

[9] SWISSto12, "Advanced antenna and RF system solutions," https://www.swissto12.ch/, 2025, accessed: Jan. 21, 2025.

[10] A. Dutt and V. Rokhlin, "Fast Fourier transforms for nonequispaced data," *SIAM Journal on Scientific Computing*, vol. 14, no. 6, pp. 1368–1393, 1993.

[11] D. Potts, G. Steidl, and M. Tasche, "Fast Fourier transforms for nonequispaced data: A tutorial," in *Modern Sampling Theory: Mathematics and Application*, J. J. B. P. Ferreira, Ed. Boston, MA: Birkhauser, 2000, pp. 253–274.

[12] K. Fourmont, "Non-equispaced fast Fourier transforms with applications to tomography," *Journal of Fourier Analysis and Applications*, vol. 9, no. 5, pp. 431–450, Sep. 2003.

[13] M. Jacob, "Optimized least-square nonuniform fast Fourier transform," *IEEE Transactions on Signal Processing*, vol. 57, no. 6, pp. 2165–2177, 2009.

[14] P. Angeletti and G. Toso, "Aperiodic arrays for space applications: A combined amplitude/density synthesis approach," in *3rd European Conference on Antennas and Propagation, EUCAP '09*, Berlin, Germany, Mar. 23-27 2009.